Available online at www.sciencedirect.com
SCIENCE DIRECT
Journal of Computational Physics 213 (2006) 437–449
JOURNAL OF COMPUTATIONAL PHYSICS
www.elsevier.com/locate/jcp

Partially reflecting and non-reflecting boundary conditions for simulation of compressible viscous flow ☆

Wolfgang Polifke [a,*], Clifton Wall [b], Parviz Moin [b]

[a] *Lehrstuhl für Thermodynamik, Technische Universität München, Boltzmannstr. 15, D-85747 Garching, Germany*
[b] *Center for Turbulence Research, Stanford University, Stanford, CA 94305, USA*

Received 31 January 2005; received in revised form 10 August 2005; accepted 17 August 2005
Available online 4 October 2005

Abstract

For numerical simulation of compressible viscous flow, the characteristics-based NSCBC boundary conditions proposed by Poinsot and Lele [T. Poinsot, S.K. Lele, Boundary conditions for direct simulation of compressible viscous flows, J. Comput. Phys. 101 (1992) 104–129] are frequently employed. This formulation is analyzed analytically and it is found that the linear relaxation term proposed by Rudy and Strikwerda [D.H. Rudy, J.C. Strikwerda, A nonreflecting outflow boundary condition for subsonic Navier–Stokes calculations, J. Comput. Phys. 36 (1) (1980) 55–70] to suppress slow "drift" of flow variables results in a non-zero reflection coefficient for acoustic waves. Indeed, although the NSCBC formulation of boundary conditions is often called "non-reflecting", the magnitude of the reflection coefficient approaches unity for low frequencies. A modification of the NSCBC boundary conditions and in particular the linear relaxation term is proposed, which should appear fully non-reflecting to plane acoustic waves with normal incidence on the boundaries for all frequencies. The new formulation is implemented and successfully validated in large eddy simulation of turbulent channel flow.

PACS: 02.70.–c; 43.20.+g; 43.60.+d; 47.11.+j; 52.35.Dm; 82.20.Wt

Keywords: Acoustics; Wave propagation and reflection; Computational fluid dynamics; Boundary conditions

1. Introduction

Acoustically non-reflecting boundary conditions for compressible (turbulent) flow simulation are a prerequisite for the successful application of computational fluid dynamics (CFD) to flow-acoustics problems, e.g., the numerical simulation of combustion instabilities. For linear problems, or for problems where linearization near the boundary is permissible, a variety of techniques have been developed, see the recent review of Colonius [1]. On the other hand, situations with nonlinear effects near the boundary – the prime example being the

☆ Expanded version of a contribution to the 11th Conference on Sound and Vibration (St. Petersburg, July 2004).

* Corresponding author. Tel.: +49 89 28916216; fax: +49 89 28916218.
E-mail addresses: polifke@td.mw.tum.de (W. Polifke), cliff.wall@gmail.com (C. Wall), moin@stanford.edu (P. Moin).

0021-9991/$ - see front matter © 2005 Elsevier Inc. All rights reserved.
doi:10.1016/j.jcp.2005.08.016

turbulent outflow problem – still pose significant problems. The Navier–Stokes characteristics boundary condition (NSCBC) developed for multi-dimensional viscous flow by Thompson, and Poinsot and Lele with the linear relaxation term proposed by Rudy and Strikwerda [2–4] has been applied successfully to many problems. However, there is evidence that this formulation, although frequently termed "non-reflecting", is indeed partly reflecting [5,6].

In this paper, the NSCBC boundary conditions are analyzed, and an analytical expression for the reflection coefficient of this formulation is derived. Then, a modification is proposed, which should allow the implementation of fully non-reflecting boundary conditions – at least for plane waves with normal incidence on the boundary. The proposed formulation is computationally very efficient and the restriction to plane waves is not a significant drawback for many applications in duct acoustics or combustion dynamics.

Both the original and the modified formulation for NSCBCs are tested in a large eddy simulation (LES) of compressible turbulent channel flow at low Mach number with external excitation. The numerical results agree with expectations except for very high frequencies (above the so-called *cut-off frequency* of the duct, i.e., the frequency of the fundamental non-plane travelling or standing acoustic mode in the duct).

In Section 2, some notation is established before characteristics based boundary conditions are reviewed briefly in Section 3. A more comprehensive discussion of the NSCBCs may be found in the original literature [2–4,7] and in textbooks [8,9]. Recent developments of the approach with extensions to real gases or mixtures thereof are discussed, for example in [10,11]. The new, non-reflecting formulation is introduced and discussed in Section 4. Results of a validation study based on large eddy simulation (LES) of compressible channel flow are shown in the last section.

2. Turbulent and acoustic fluctuations, characteristic wave amplitudes

When dealing with problems of compressible turbulent flow, it is often advantageous to distinguish conceptually between turbulent ("′") and acoustic ("∼") fluctuations of the flow variables, e.g.,

$$p(\vec{x},t) = \bar{p}(\vec{x}) + \tilde{p}(x,t) + p'(\vec{x},t), \tag{1}$$

$$u(\vec{x},t) = \bar{u}(\vec{x}) + \tilde{u}(x,t) + u'(\vec{x},t) \tag{2}$$

for the pressure and the x-component of velocity, respectively. The overbar denotes mean values. In this paper, we are concerned primarily with plane acoustic waves. Without essential loss of generality, it is assumed that the waves propagate in the x-direction, as shown in Fig. 1. Therefore, the acoustic signal components $\tilde{p}$ and $\tilde{u}$ in the above equations depend only on the the x-component of the position $\vec{x}$.

2.1. Characteristic wave amplitudes

Given that perturbation amplitudes are sufficiently small, acoustic signal components are conveniently expressed in terms of the (linearized) characteristic wave amplitudes $f = f(x - (\bar{u} + \bar{c})t)$ and $g = g(x - (\bar{u} - \bar{c})t)$, traveling in the positive and negative x-direction, respectively (see again Fig. 1). Characteristic wave amplitudes f, g and acoustic fluctuations of pressure p' and velocity u' are related to each other as follows:

$$\frac{\tilde{p}}{\bar{\rho}\bar{c}} = f + g, \quad \tilde{u} = f - g \tag{3}$$

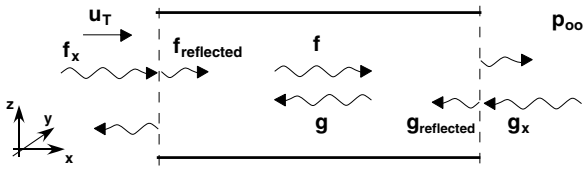

Fig. 1. Domain with characteristic waves f, g in the interior and at the boundaries. $f_{\text{reflected}}$, $g_{\text{reflected}}$: reflected waves at the upstream inlet and at the downstream outlet boundary, respectively. f_x, g_x: external forcing at inlet and outlet, respectively (cf. Section 3.2.4).

and conversely

$$f = \frac{1}{2}\left(\frac{\tilde{p}}{\bar{\rho}\bar{c}} + \tilde{u}\right), \quad g = \frac{1}{2}\left(\frac{\tilde{p}}{\bar{\rho}\bar{c}} - \tilde{u}.\right). \tag{4}$$

For harmonic waves with angular frequency ω

$$f(x,t) = \hat{f}\mathrm{e}^{\mathrm{i}(\omega t - k_{x+}x)}, \quad g(x,t) = \hat{g}\mathrm{e}^{\mathrm{i}(\omega t - k_{x-}x)}. \tag{5}$$

Here, $k_{x\pm} \equiv \pm\omega/\bar{c}(1 \pm M)$ are the wave numbers of the invariants, the "$\hat{}$" indicates a complex-valued wave amplitude, and $M \equiv \bar{u}/\bar{c}$ is the Mach number of the mean flow. The above relations can be obtained by linearization of the acoustic equations about the mean flow.

2.2. Identification of acoustic signal components

To analyze the propagation and reflection of acoustic waves in compressible flow simulation, one must be able to determine the acoustic signal components, i.e., the wave amplitudes f, g from flow variables $u(\vec{x},t)$ and $p(\vec{x},t)$. Referring to Eqs. (1) and (2), it is obvious that this is not a trivial problem, because in DNS or LES of turbulent flow, turbulent contributions u' and p' to the velocity or pressure signals can be significant and must be distinguished from the acoustic components $\tilde{p}$ and $\tilde{u}$. In this paper, we are primarily interested in propagation of plane waves in a duct at low frequencies (below the cut-off frequency of higher order, non-plane modes, say) and therefore propose to exploit:

(1) scale separation;
(2) spatial symmetries;
(3) the inherent coupling between pressure and velocity fluctuations in traveling acoustic waves to differentiate between turbulent and acoustic signal contributions.

For this purpose, an (instantaneous) area average $\langle\cdots\rangle$ over sampling planes perpendicular to the duct axis is introduced. Plane acoustic waves travelling along the duct exhibit – with the exception of the acoustic boundary layer, which is usually very thin – no spatial variation over such sampling planes, so

$$\langle f\rangle \approx f \quad \text{and} \quad \langle g\rangle \approx g.$$

On the other hand, if the spatial correlation length of turbulent eddies (the turbulent length scale) is sufficiently small, then the area average over turbulent fluctuations will almost vanish,

$$\langle u'\rangle \approx 0 \quad \text{and} \quad \langle p'\rangle \approx 0.$$

It is therefore proposed to *identify* acoustic signal components as follows:

$$f = \frac{1}{2}\left(\frac{\delta p}{\bar{\rho}\bar{c}} + \delta u\right) \text{ for a plane wave propagating downstream,} \tag{6}$$

$$g = \frac{1}{2}\left(\frac{\delta p}{\bar{\rho}\bar{c}} - \delta u\right) \text{ for a plane wave propagating upstream} \tag{7}$$

with deviations

$$\delta u \equiv \langle u - \overline{u}\rangle, \quad \delta p \equiv \langle p - \overline{p}\rangle \tag{8}$$

from the mean values. This form makes explicit that acoustic waves comprise fluctuations of both velocity and pressure.

3. Boundary conditions in compressible viscous flow

Consider a (computational) domain as shown in Fig. 1, with acoustic signals f, g travelling back and forth. At the domain boundaries, acoustic waves are partly reflected (outgoing and reflected components are indicated in the figure). Furthermore, there may be external acoustic excitation signals f_x or g_x at the inflow and outflow boundary, respectively.

Boundary conditions in compressible viscous flow simulation must fulfill several requirements:

(1) a target velocity u_T at the inlet as well as a far-field pressure p_∞ at the outlet must be imposed. Note that for direct or large eddy simulation of turbulent flows, the target velocity must comprise a fluctuating turbulent signal component, i.e., $u_T = \bar{u} + u'$;
(2) for some applications it is required that external excitation signals f_x or g_x of suitable amplitude and frequency content be imposed [12,13] such that a significant acoustic signal can be detected;
(3) for many applications it is required that outgoing waves leave the domain without reflection [5,12,14].

As explained below, these requirements are to some extent conflicting. Therefore it is not surprising that many different formulations for boundary conditions have been developed [1–4,8,9]. Most formulations are "special purpose", i.e., they can only be applied to certain flow regimes or flow configurations, or they fulfill one of the above requirements particularly well, while exhibiting deficits or disadvantages in some other respect. Furthermore, boundary treatments can be computationally quite expensive, e.g., if they require an enlarged computational domain ("sponge region"). This is not acceptable for some computationally demanding applications. One may conclude that a completely general formulation has not yet been developed.

The modified NSCBC formulation presented in this paper is suited to problems of duct acoustics and in particular combustion instabilities [12,13,15,16], where often plane wave propagation below the so-called "cut-off frequency" (of higher-order, non-plane acoustic modes) is of particular importance.

To introduce notation and fundamental ideas, the original NSCBC formulation of Poinsot and Lele [3] is reviewed very briefly in the next subsection. Then it is discussed how and to which extent the requirements (1)–(3) are satisfied by this treatment. Detailed background information on the NSCBC formulation is available in journal publications and monographs [2–4,6,8,9].

3.1. Wave amplitude variations and LODI relations

If the boundary lies in the (y, z)-plane, say, (see Fig. 1) the boundary conditions for plane waves travelling in the x-direction are formulated with the help of two quantities $\mathscr{L}_5$ and $\mathscr{L}_1$

$$\mathscr{L}_i \equiv \lambda_i \left(\frac{\partial p}{\partial x} \pm \bar{\rho}\bar{c} \frac{\partial u}{\partial x} \right), \tag{9}$$

where the "+"-sign corresponds to the index "5", and the propagation speeds are denoted as $\lambda_i \equiv u \pm c$. According to [3], the $\mathscr{L}_i$'s can be interpreted as the temporal rate of change of wave amplitudes at the boundary and are therefore referred to as *wave amplitude variations*.

To obtain approximate values for the wave amplitude variations $\mathscr{L}_i$ in terms of the primitive flow variables, so-called *local one-dimensional inviscid* (LODI) relations are introduced [3]. For pressure and the velocity component normal to the boundary

$$\frac{\partial p}{\partial t} + \frac{1}{2}(\mathscr{L}_5 + \mathscr{L}_1) = 0, \tag{10}$$

$$\frac{\partial u}{\partial t} + \frac{1}{2\bar{\rho}\bar{c}}(\mathscr{L}_5 - \mathscr{L}_1) = 0. \tag{11}$$

The values of flow variables at the boundaries at time step $n+1$ can be computed with the help of these relations from the flow variables and wave amplitude variations at time step n. For example, using an explicit Euler time stepping scheme and p, u as flow variables

$$p^{(n+1)} = p^{(n)} - \frac{\Delta t}{2}\left(\mathscr{L}_5^{(n)} + \mathscr{L}_1^{(n)} \right), \tag{12}$$

and similarly for the velocities [2]. Alternative choices for the flow variables and alternative time stepping schemes – resulting in a different formulation of the right hand side of the above equation – have been proposed [3], but these differences are not essential in the present context.

For acoustic fluctuations, the corresponding wave amplitude variations $\mathscr{L}$ and the LODI relations can be expressed in terms of the wave amplitudes f, g. Recalling the definitions (4) and (9) and subtracting Eqs. (10) and (11) from each other, one obtains easily

$$\frac{\partial}{\partial t}\left(\frac{\tilde{p}}{\bar{\rho}\bar{c}} \pm \tilde{u}\right) + \frac{1}{\bar{\rho}\bar{c}}\mathscr{L}_i = 0, \tag{13}$$

with $i = 5$ for the "+"-sign and $i = 1$ for the "−"-sign, respectively. In the present context, plane harmonic waves are of particular interest. Using "$\hat{.}$" to denote the Fourier coefficient of a quantity, we find

$$\hat{\mathscr{L}}_1 = -\mathrm{i}2\omega\bar{\rho}\bar{c}\hat{g}, \tag{14}$$

$$\hat{\mathscr{L}}_5 = -\mathrm{i}2\omega\bar{\rho}\bar{c}\hat{f}. \tag{15}$$

3.2. (Partially) reflecting boundary conditions

In this section various types of characteristics-based boundary conditions, as they can be implemented in the NSCBC framework, are reviewed and their acoustic properties are briefly recapitulated. This discussion is meant to clarify the properties and the limitations of the standard NSCBC formulation, and it should prepare the ground for modified NSCBC formulation proposed in this paper.

3.2.1. Fully reflecting boundary – "open end" and "closed end"

At a subsonic reflecting outlet, which corresponds to an "open end" boundary condition in acoustics, $\tilde{p} = f + g = 0$. The acoustic reflection factor r, defined as the amplitude ratio of reflected and outgoing acoustic waves, equals

$$r \equiv \frac{\hat{g}}{\hat{f}} = -1. \tag{16}$$

Of course, this definition of the reflection coefficient physically makes sense only if there is no incoming acoustic excitation signal g_x. From the results of the last section, we infer for acoustic fluctuations that $\mathscr{L}_1 + \mathscr{L}_5 = 0$ at an "open end".

A fully reflecting "closed end" inflow boundary condition with $\tilde{u} = f - g = 0$ and $r \equiv \hat{f}/\hat{g} = 1$ may be defined in an entirely analogous manner.

3.2.2. Partially reflecting boundary with linear relaxation term

If the temporal evolution of pressure or velocity at a (subsonic) boundary would be determined solely from an outgoing wave $\mathscr{L}_i$ via the appropriate LODI relation (10) or (11), then – neglecting viscous and multidimensional effects – the outgoing wave would leave the domain without reflection. A boundary condition constructed in this manner would exhibit a zero reflection coefficient, which would be very convenient for many applications.

However, as explained above, target values of pressure p_∞ or velocity u_T, respectively, must be imposed at the boundary. To this purpose, Rudy and Strikwerda have introduced a "linear relaxation term", which generates a corrective signal whenever velocity or pressure deviate from the respective target value [4].

At an outlet, say, where the boundary condition has to maintain pressure, Poinsot and Lele formulate such a corrective signal in terms of the wave amplitude variation $\mathscr{L}_1$

$$\mathscr{L}_1 = \frac{\sigma\bar{c}}{L}(p - p_\infty), \tag{17}$$

where σ is a coupling parameter and the speed of sound c and length L are introduced for dimensional consistency [3]. Then, if there is no outgoing acoustic wave $\mathscr{L}_5$, we see with (10) that an excess pressure $\Delta p = p - p_\infty$will be reduced exponentially to zero according to

$$\frac{\partial \Delta p}{\partial t} = -\frac{\sigma\bar{c}}{2L}\Delta p, \tag{18}$$

with a decay time τ inversely proportional to the coupling coefficient σ

$$\tau \equiv \frac{2L}{\sigma \bar{c}}. \tag{19}$$

At an inlet, the velocity u_T has to be imposed. If a relaxation term

$$\mathscr{L}_5 = \frac{\sigma \bar{c}}{L} \bar{\rho} \bar{c} (u - u_T), \tag{20}$$

is introduced, one finds with the LODI relation (11) that again any deviation of the inflow velocity from the target value u_T should decay exponentially with a time constant $2L/\sigma\bar{c}$.

At least for problems without essential nonlinearities, LODI-based boundary conditions with relaxation terms (17) or (20) have been found to work well in practice, provided that the coupling parameters σ are large enough. If the coupling is too weak, a slow "drift" of pressure or overall mass flow rate from the target value and even divergence of the flow solver is observed.

3.2.3. Reflecting coefficient of boundaries with a linear relaxation term

A boundary condition constructed in this manner is unfortunately no longer fully non-reflecting to acoustic waves, because outgoing acoustic waves f (at an outlet) and g (at an inlet) contribute to the primitive flow variables p and u, which appear in the relaxation terms (17) and (20). As a consequence, the outgoing waves are to some extent reflected back into the computational domain.

Magnitude and phase of the reflection coefficient r of characteristics-based boundary conditions with relaxation term can be estimated if one assumes that a sufficiently large value for the coupling parameter σ has been chosen such that drift of pressure or velocity is effectively suppressed. Then deviations from the target pressure at an outlet, say, will be dominated by acoustic signals

$$\tilde{p} = \langle p - p_\infty \rangle.$$

A reflected wave will be generated by the coupling term due to this deviation from the target value. Using relations (14) and (17) one estimates for the reflection coefficient

$$r(\omega) \equiv \frac{\hat{g}}{\hat{f}} = \frac{\langle \hat{\mathscr{L}}_1 \rangle}{-\mathrm{i}2\omega\bar{\rho}\bar{c}\hat{f}} = \frac{\sigma\bar{c}\langle \hat{p} \rangle / L}{-\mathrm{i}2\omega\bar{\rho}\bar{c}\hat{f}}. \tag{21}$$

We are assuming that pressure fluctuations around the target value are dominated by acoustic waves f, g, and with the definition (4) we rewrite the r.h.s. of the above equation as follows:

$$\frac{\mathrm{i}\sigma\langle \hat{p} \rangle}{2L\omega\bar{\rho}\hat{f}} = \frac{\mathrm{i}\sigma\bar{c}}{2L\omega} \frac{\hat{f} + \hat{g}}{\hat{f}} = \frac{\mathrm{i}}{\omega\tau}(1 + r). \tag{22}$$

Combining the last two equations and solving for r, a complex-valued reflection coefficient is obtained

$$r(\omega) = \frac{-1}{1 + \mathrm{i}\omega\tau} = \begin{cases} 0 & \text{for } \omega\tau \to \infty \text{ (high-frequency limit)}, \\ -1 & \text{for } \omega\tau \to 0 \text{ (low-frequency limit)}. \end{cases} \tag{23}$$

For waves with relatively high frequency – with a period of oscillation much smaller than the decay constant τ – the restoration of the pressure at the outlet according to (17) is too slow to respond to the acoustic perturbations, such that the boundary is indeed effectively non-reflecting. Note that the phase of the reflection coefficient approaches $\pi/2$ in the high-frequency limit.

Conversely, a low frequency signal is reflected as if it had encountered an "open end" ($\tilde{p} = 0$), because the boundary condition (17) succeeds in keeping the pressure at the outlet close to the target value p_∞ due to the comparatively short decay time constant τ.

This result should be valid provided that:

- harmonic waves dominate the deviations from the target pressure;
- the frequency ω is non-zero;
- there is no external excitation signal g_x.

The reflection coefficient for a flow inlet with linear relaxation term according to (20) may be estimated in an entirely analogous manner. One obtains

$$r(\omega) = \frac{\hat{f}}{\hat{g}} = \frac{1}{1 + \mathrm{i}\omega\tau} = \begin{cases} 0 & \text{for } \omega\tau \to \infty \text{ (high-frequency limit)}, \\ 1 & \text{for } \omega\tau \to 0 \text{ (low-frequency limit)}. \end{cases} \tag{24}$$

i.e., in the low-frequency limit the boundary condition (20) acts like a "closed end" without fluctuations of velocity.

The absolute value $|r|$ of the reflection coefficient – which is the same for (23) and (24) – is plotted in Fig. 2 vs. $\omega\tau$, i.e., angular frequency non-dimensionalized with the time constant τ of the coupling relation, see Eqs. (18)–(20). Clearly, the boundary conditions (17) and (20) lead to significant reflection of outgoing waves for low frequencies and or for large values of the coupling coefficient σ (i.e., for small values of $\omega\tau = 2\omega L\sigma\bar{c}$).

If the magnitude of the reflection coefficient $|r|$ is not to exceed a certain value for a given frequency ω, then the corresponding minimum time constant τ and thereby the maximum coupling coefficient σ can be deduced from this plot. Unfortunately, if the coupling coefficient σ is set below a certain value, divergence of the flow solver or "drift" of velocity or pressure from the target values u_T and p_∞, respectively, are observed. It follows that boundaries with arbitrarily low reflection coefficient at low frequencies, let alone fully non-reflecting boundaries, cannot be implemented with the formulation developed by Rudy and Strikwerda [4] and Poinsot and Lele [3]. Note that Selle et al. [6] have obtained results equivalent to (23) and (24) by analyzing a differential equation for pressure perturbations resulting from Eqs. (17) and (20).

3.2.4. External acoustic excitation

With the help of (14) and (15), wave amplitudes $\tilde{\mathscr{L}}_1$ and $\tilde{\mathscr{L}}_5$ representing external acoustic excitations signals f_x and g_x can be specified as additional terms in the boundary conditions

$$\mathscr{L}_i = \cdots + \tilde{\mathscr{L}}_i, \tag{25}$$

where "$\cdots$" stands for the coupling terms discussed above (see Eqs. (17) or (20)), or terms which correspond to inflow turbulence. For example, if the incoming signal is a superposition of sine-waves (as used below), then the corresponding wave amplitude variation equals

$$\tilde{\mathscr{L}}_5 = -2\bar{\rho}\bar{c}\sum A_n\omega_n\cos(\omega_n t + \phi_n). \tag{26}$$

Alternatively, if a random number generator and a Butterworth filter are used to generate a "'white noise" time series $f_x(t)$ with uniform power spectral density over a certain range of frequencies, then according to (14) the time derivative of this series provides the related wave amplitude variation $\tilde{\mathscr{L}}_5$

$$\tilde{\mathscr{L}}_5 = -2\bar{\rho}\bar{c}\frac{\partial f_x(t)}{\partial t}. \tag{27}$$

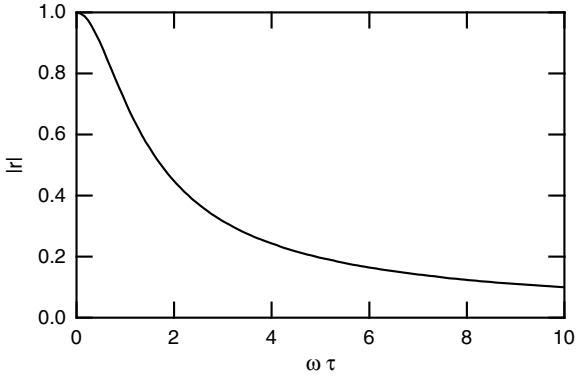

Fig. 2. Absolute value of reflection coefficient $|r|$ vs. non-dimensional frequency $\omega\tau$ for partially reflecting in- or outflow boundary condition according to (17) and (20).

4. Non-reflecting boundary conditions with plane-wave "masking"

It is possible to construct characteristics-based boundary conditions, which – at least for plane acoustic waves with normal incidence – should be nearly non-reflecting even for low frequencies $\omega\tau \to 0$. The idea is to *identify* outgoing plane waves at the boundary, and then explicitly eliminate outgoing wave contributions from the linear relaxation term.

For example, at an outflow boundary the pressure coupling (17) would be modified as follows:

$$\mathscr{L}_1 = \frac{\sigma\bar{c}}{L}(p - \bar{\rho}\bar{c}f - p_\infty). \tag{28}$$

In this way the contribution of the outgoing wave f to the pressure p is removed from the linear relaxation term. In other words, the "masked" outgoing wave f no longer contributes to the incoming wave $\mathscr{L}_1$ and therefore should leave the domain without reflection at the boundary.

A modified velocity coupling term (20) at an inflow boundary is formulated in an analogous manner

$$\mathscr{L}_5 = \frac{\sigma\bar{c}}{L}\bar{\rho}\bar{c}(u + g - u_\mathrm{T}). \tag{29}$$

4.1. Identification of outgoing waves at the boundary

To make the proposed scheme for non-reflecting boundary conditions work, outgoing wave amplitudes f, g in (28) and (29) must be determined from the flow variables $u(\vec{x},t)$ and $p(\vec{x},t)$ at or near the boundary.

It is proposed to use the approach described in Section 2.2 for post-processing of computational data, i.e., to compute area averages $\langle\cdots\rangle$ over the boundary plane and identify the outgoing plane wave components via the relations (6) and (7) as deviations

$$\delta u \equiv \langle u - \overline{u}\rangle, \tag{30}$$

$$\delta p \equiv \langle p - \overline{p}\rangle \tag{31}$$

from the mean or target values of velocity and pressure, respectively.

4.2. Reflection coefficient with plane wave masking

Using again area averages $\langle\cdots\rangle$, the reflection coefficient resulting from the boundary conditions (28) and (29) with plane wave masking can be estimated. At an outflow boundary, say, the reflected wave g is determined with Eq. (14) from the wave amplitude variation $\mathscr{L}_1$

$$r(\omega) = \frac{\langle\hat{g}\rangle}{\langle\hat{f}\rangle} = \frac{\langle\hat{\mathscr{L}}_1\rangle}{-2\mathrm{i}\omega\bar{\rho}\bar{c}\langle\hat{f}\rangle}. \tag{32}$$

Inserting the expression for $\mathscr{L}_1$ as it results from the boundary condition (28), one finds

$$r(\omega) = \frac{\frac{\sigma c}{L}\langle\hat{p} - \bar{\rho}\bar{c}\hat{f} - \hat{p}_\infty\rangle}{-2\mathrm{i}\omega\bar{\rho}\bar{c}\langle\hat{f}\rangle} = \frac{\mathrm{i}\sigma c}{2\omega L\langle\hat{f}\rangle}\left(\frac{\langle\hat{p} - \hat{p}_\infty\rangle}{\bar{\rho}\bar{c}} - \langle\hat{f}\rangle\right). \tag{33}$$

Here, it has been made explicit that the outgoing characteristic wave amplitudes f is estimated from area-averages, although we expect – as discussed in Section 2.2 – that $\langle f\rangle \approx f$ (and similarly for g at an inflow).

It has been argued above that with sufficient scale separation between turbulent and acoustic fluctuations, area-averaged deviations δp of pressure from the target value p_∞ should be caused only by plane acoustic waves. In this case

$$\frac{\langle p - p_\infty\rangle}{\bar{\rho}\bar{c}} = f$$

at the boundary and it follows from (33) that the reflection coefficient should indeed vanish *by construction*:

$$r(\omega) \approx 0$$

for plane harmonic waves of arbitrary non-zero frequency.

Similar arguments suggest that an inflow boundary condition according to (29) would also be non-reflecting even at very low frequencies. Again, this result rests on the assumption that area-averaged deviations δu of velocity from the target value u_T are primarily due to outgoing acoustic waves, $\langle u - u_T \rangle = -g$.

4.3. Drift of average pressure or velocity with plane wave masking

Is it possible that the average values of flow variables at the boundaries drift away from the prescribed values p_∞ and u_T, respectively, because the "masking" of plane waves in (28) and (29) hides the drift from the linear relaxation term?

If the coupling coefficient σ at on outlet, say, is too small to suppress pressure drift, one usually observes that the deviation Δp of pressure from the physically correct value grows slowly throughout the computational domain. In this situation, area averaging cannot suppress the spurious identification of the pressure drift as an acoustic signal, because $\delta p = \langle \Delta p \rangle \approx \Delta p$.

Fortunately, this pressure fluctuation due to drift is not accompanied by a corresponding velocity fluctuation – as it would be in a true acoustic wave. Indeed constant overall mass flux and therefore $\delta u = 0$ has been observed whenever pressure drift occurred in one of the large eddy simulation runs performed in the course of this study (not shown).

It follows that according to (6) a spurious outgoing characteristic wave amplitude f is identified:

$$f = \frac{1}{2}\left(\frac{\delta p}{\bar{\rho}\bar{c}} + \delta u\right) = \frac{\Delta p}{2\bar{\rho}\bar{c}}. \tag{34}$$

Inspecting the modified boundary conditions (28), we find that

$$\mathscr{L}_1 = \frac{\sigma\bar{c}}{L}\left((p_\infty + \Delta p) - \bar{\rho}\bar{c}f - p_\infty\right) = \frac{\sigma\bar{c}}{2L}\Delta p, \tag{35}$$

i.e., the ingoing wave amplitude variation generated to correct the drift is only half as strong as it was previously (see Eq. (18)). Nevertheless, one may conclude that despite the spurious identification of an outgoing wave amplitudes, the modified linear relaxation term restores the target pressure, although the time constant τ is now twice as large as for the standard formulation.

It may be shown in an analogous manner that a deviation of the velocity u from the target value at an inlet would be reduced to zero by with a time constant twice as large as for the partially reflection inflow boundary condition (20).

4.4. Acoustic excitation with plane wave masking

It is straightforward to construct non-reflecting boundaries with masking of outgoing plane waves and acoustic excitation, because incoming wave amplitudes f_x at the upstream inlet and g_x at the downstream outlet boundary, respectively, are known by construction.

At an outflow, say, the boundary condition (28) would be modified as follows:

$$\mathscr{L}_1 = \frac{\sigma\bar{c}}{L}\left(p - \bar{\rho}\bar{c}(f + g_x) - p_\infty\right) + \tilde{\mathscr{L}}_1. \tag{36}$$

The motivation for the explicit appearance of the excitation signal g_x in the modified relaxation term is the following: excitation is imposed by the incoming wave amplitude variation $\tilde{\mathscr{L}}_1$, cf. Eq. (25). Any additional contributions to $\mathscr{L}_1$, which may be generated by g_x contributing to the linear relaxation term, must be considered as spurious and should therefore be eliminated. This is simply achieved by explicitly subtracting the contribution of g_x to the pressure p at the boundary.

A modified non-reflecting inflow boundary with excitation is formulated in an analogous manner

$$\mathscr{L}_5 = \frac{\sigma\bar{c}}{L}\bar{\rho}\bar{c}\left(u - (f_x - g) - u_T\right) + \tilde{\mathscr{L}}_5. \tag{37}$$

5. Simulation results

Large eddy simulation of a channel flow configuration at a Reynolds number based on channel height, H, and bulk velocity, U_b, of 25,000 and a Mach number based on bulk velocity of 3.3×10^{-2} has been performed to validate the non-reflective character of the new boundary conditions. The length, L, of the computational domain was twenty channel heights H, and the width, W, was three channel heights. No slip conditions were applied at the top and bottom walls of the channel, and periodic boundary conditions were applied at the spanwise boundaries. A grid of $128 \times 64 \times 32$ points in the streamwise, wall normal, and spanwise directions, respectively, was used for the simulations. The time step for the simulation was $10^{-3} H/U_b$. The turbulence model used was the dynamic model of Moin et al. [17] for compressible turbulence. The numerical formulation was the method of Wall et al. [18], which is an extension of the method of Pierce [19] to compressible flow. It is efficient at low Mach number without introducing any artificial damping of acoustic waves.

The dissipation parameter that is described by Wall et al. [18] was set to zero. This method is second order accurate in space and time. The discretization is also centered in both space and time, resulting in no artificial dissipation of acoustic waves. Turbulent inflow date for u′ as well as the wall normal and spanwise components of velocity at the inlet plane were obtained from a separate, incompressible, channel flow calculation using the method of Pierce and Moin [20].

Simulations with harmonic forcing at several frequencies ω_i at the upstream (inflow) boundary have been carried out. The lowest (angular) frequency $\omega_1 \approx 2.5$ (non-dimensionalized with flow speed and channel height) with wave length $\lambda \approx 80$ would correspond to a quarter-wave mode along the length of the channel. The highest excitation frequencies shown are significantly above the cut-off frequencies $\omega_c \approx 60$ for higher-order, non-plane acoustic modes. At each time step, the code outputs the instantaneous values of both pressure $\langle p \rangle$ and streamwise velocity $\langle u \rangle$ close to the boundaries of the computational domain. These values are computed as area-averages over sampling planes oriented perpendicular to the mean flow direction at positions $x/H = 0.1$ and $x/H = 19.9$, respectively. The characteristic wave amplitudes f, g are computed from the flow variables $\langle p \rangle$ and $\langle u \rangle$ using the relations (4), (6) and (7).

5.1. Results for the outflow boundary

For the simulations discussed in this subsection, forcing and masking according to (26) and (37) have been employed at the inflow boundary. At the outflow, the standard formulation (17) and the new formulation (36) with masking have been used, respectively. Results obtained with the two different outflow boundary conditions are compared against each other in Figs. 3 and 4. The coupling coefficient σ has been set to $\sigma \bar{c}/L = 165$ at both boundaries. This is the minimum value required to avoid pressure drift for the present simulations.

The power spectral distributions (PSDs) for the two simulations without (left) and with (right) masking are shown in Fig. 3. The amplitudes of the waves f_d approaching the boundary are obviously of the same order of magnitude, while the amplitude of reflected waves $g_{\text{reflected}}$ is much smaller for the simulation with masking (middle left vs. middle/right graphs). The bottom row of graphs shows an outflow "reflection coefficient" $|\hat{r}| = |\hat{g}/\hat{f}|$ for frequencies in the range $\omega = 0.628, \ldots, 340$. This quantity is much smaller for the boundary condition with masking at low frequencies, while at high frequencies both formulations yield $|\hat{g}/\hat{f}| \approx 0.5$.

However, it does not make sense to interpret $\hat{g}/\hat{f}$ as an acoustic reflection coefficient at frequencies where there is no acoustic forcing – because at those frequencies there is no acoustic wave to reflect. Therefore, in Fig. 4 reflection coefficients are plotted only at those frequencies where external forcing is imposed. A log-scale is used for the abscissa, such that the results for the lower frequencies are better visible. In this representation it is very clear that indeed the standard formulation (17) is fully reflecting at low frequencies. Also shown in Fig. 4 is the analytical estimate (23) for the reflection coefficient. It obviously agrees rather well with the numerical result up to frequencies exceeding the cut-off frequency of higher order modes; $\omega_c \approx 60$ for the present channel geometry.

Plane wave masking, on the other hand, produces very small reflection factors $|r| \to 0$ for low frequencies (recall that for the computational setup chosen $\omega = 2.5$ corresponds to the "quarter-wave" mode of the duct). For higher frequencies, the reflection factor obtained with plane wave masking increases significantly.

In our opinion, the difficulty to distinguish properly between turbulent and acoustic signal components in the LES computation is to be held accountable for the discrepancies observed at higher frequencies. In

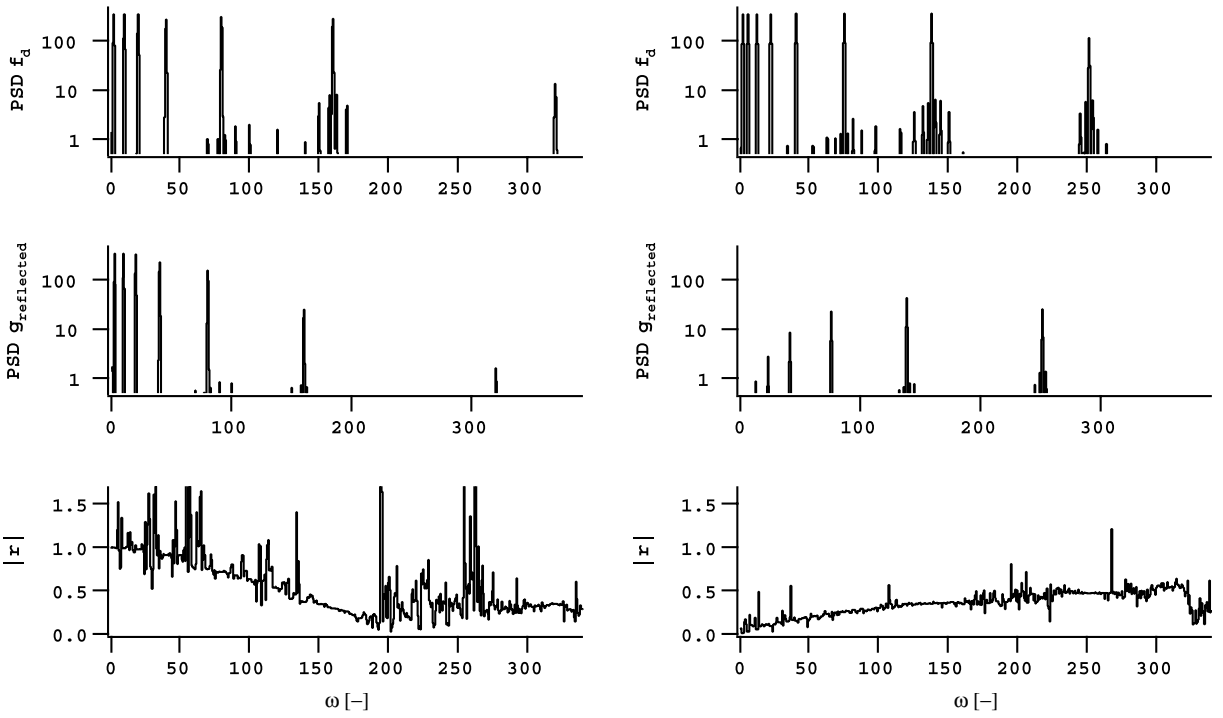

Fig. 3. LES Results with upstream harmonic forcing at discrete frequencies ω_i. (Top) Power spectral density (PSD) of outgoing wave f_d; (Middle) PSD of reflected wave g_d; (Bottom) reflection coefficient $r(\omega) \equiv |g/f|$. (Left) Standard characteristics based BCs, see Eq. (17). (Right) With plane wave masking, see Eq. (36).

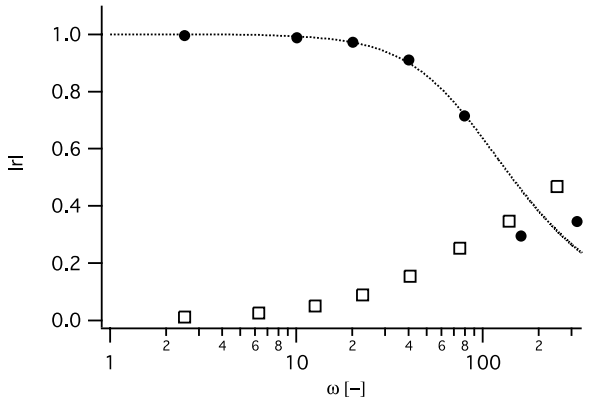

Fig. 4. Reflection coefficient of outflow boundary as observed in LES without plane wave masking (●, see Eq. (17)), with plane wave masking (□, see Eq. (36)) and according to the approximate theoretical analysis presented above (···, see Eq. (23)).

this frequency range, the scale separation between acoustic and turbulent fluctuations weakens. Consequently, the "measurement" of the characteristic wave amplitudes f, g as well as the reflection factor r is severely disturbed by turbulent contributions u' and p' to the fluctuations of the flow variables. The observation that the magnitude of the reflection factor approaches for high frequencies a value of roughly 0.5 no matter what boundary formulation is used (see also Fig. 5) supports this argument. Furthermore, the modified NSCBC boundary treatment with "masking" relies on proper identification of outgoing acoustic waves at the boundary. The simple identification procedure employed in this study – see Eq. (6) – is also based on deviations δu and δp from area averages and may no longer be adequate for higher

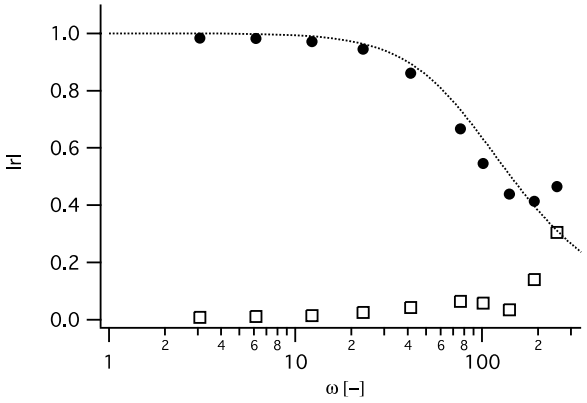

Fig. 5. Reflection coefficient of inflow boundary as observed in LES without plane wave masking (●, see Eq. (20)), with plane wave masking (□, see Eq. (37)), and according to the analysis presented in Section 3.2.2 (···, see Eq. (24).

frequencies, resulting in non-zero reflection coefficients. A recently proposed characteristics-based filter for acoustic signal identification in LES should alleviate these problems [21].

Computational results of Selle et al. [6], using the linear restoring term without plane wave masking – the "partially reflecting boundary condition", see Eq. (17) – lend further support to this interpretation of the results at higher frequencies: Selle et al. studied laminar compressible flow, so there were no turbulent signal contributions to the reflection coefficients measured. Indeed, perfect agreement could be observed for a wide range of frequencies between the analytical estimate (23) for the reflection coefficient of the standard formulation of NSCBC boundary conditions and the simulation results.

5.2. Results for the inflow boundary

Additional simulations have been performed to confirm that the novel formulation also works at an inflow boundary. Harmonic forcing and masking has been imposed at the downstream outflow boundary. At the inlet, both the standard formulation (20) and the new formulation (37) with masking have been used. The coupling coefficient σ has again been set to $\sigma\bar{c}/L = 165$ at both boundaries. The reflection coefficients for these two simulations observed at the inflow boundary are compared against each other in Fig. 5.

6. Summary and outlook

The characteristics-based NSCBC formulation of boundary conditions for simulation of turbulent compressible flows was originally proposed as a "non-reflecting" boundary condition [3]. However, in the present work it was shown that the standard formulation with a linear relaxation term is in general partially reflecting and indeed strongly reflecting for large coupling coefficients or low frequencies.

For plane acoustic waves with normal incidence on the boundary, it is possible to quantify analytically the frequency dependence of the reflection coefficient $r(\omega)$ of the standard NSCBC. Our analysis corroborates the results of Selle et al. [6] and has been largely confirmed by large eddy simulation of turbulent channel flow.

A modification of the NSCBC boundary conditions with "wave masking" has been introduced, which by construction should be fully non-reflecting at low frequencies. This formulation is computationally efficient and does not require an artificially enlarged computational domain. The NSCBC with wave masking has been implemented and validated with large eddy simulation of compressible turbulent channel flow at low Mach number. At least for very low frequencies, near-zero reflection coefficients were observed without drift of overall mass flux or system pressure. Non-zero reflection coefficients at frequencies significantly above the cut-off frequency for non-plane waves are attributed to imperfect identification of acoustic signal components in turbulent flow simulation.

In its present form, the modified formulation with wave masking is applicable to plane acoustic waves with normal incidence on the boundaries of the computational domain. This entails that the relevant acoustic fre-

quencies must not be too high, and indeed should be below the cut-off frequency of non-plane acoustic modes. Furthermore, the computational domain should have straight inlet and outlet sections aligned with the direction of wave propagation. However, these restrictions do certainly not imply that the modified formulation with wave masking is only applicable to channel flow. For example, the method has been applied with good success to the simulation of thermo-acoustic combustion instabilities in a premix combustor test rig [22,23].

Acknowledgments

The ideas presented in this work were developed during the 2002 Summer Program of the Center for Turbulence Research (CTR) at NASA Ames Research Ctr./Stanford University [13]. Discussions with Summer Program participants and CTR staff, in particular Andre Kaufmann, Thierry Poinsot, Laurent Selle and Sanjiva Lele are gratefully acknowledged. Thanks to Andreas Huber for proof-reading and helpful suggestions. Financial support was provided by Alstom Power and Siemens Power Generation in the framework of the AG Turbo Programme (German Ministry for Education and Research) as well as by the Center for Turbulence Research.

References

[1] T. Colonius, Modeling artificial boundary conditions for compressible flow, Annu. Rev. Fluid Mech. 36 (2004) 315–345.
[2] K.W. Thompson, Time dependent boundary conditions for hyperbolic systems, J. Comput. Phys. (68) (1987) 1–24.
[3] T. Poinsot, S.K. Lele, Boundary conditions for direct simulation of compressible viscous flows, J. Comput. Phys. (101) (1992) 104–129.
[4] D.H. Rudy, J.C. Strikwerda, A nonreflecting outflow boundary condition for subsonic Navier–Stokes calculations, J. Comput. Phys. 36 (1) (1980) 55–70.
[5] T. Schönfeld, T. Poinsot, Influence of boundary conditions in LES of premixed combustion instabilities, Annual Research Briefs, Center for Turbulence Research, Stanford, CA, 1999.
[6] L. Selle, F. Nicoud, T. Poinsot, Actual impedance of nonreflecting boundary conditions: implications for computation of resonators, AIAA J. 42 (5) (2004) 958–964.
[7] M. Giles, Non-reflecting boundary conditions for Euler equation calculations, AIAA J. 28 (12) (1990) 2050–2058.
[8] T. Poinsot, D. Veynante, Theoretical and Numerical Combustion, second ed., Edwards, R.T., Philadelphia, PA, USA, 2005.
[9] E.S. Oran, J. Boris, Numerical Simulation of Reactive Flow, Appleton & Lange, New York, 1987.
[10] V. Moureau, G. Lartigue, Y. Sommerer, C. Angelberger, O. Colin, T. Poinsot, High-order methods for DNS and LES of compressible multi-component reacting flows on fixed and moving grids, J. Comput. Phys. 202 (2005) 710–736.
[11] N. Okong'o, J. Bellan, Consistent boundary conditions for multicomponent real gas mixtures based on characteristic waves, J. Comput. Phys. 176 (2002) 330–344.
[12] A. Kaufmann, F. Nicoud, T. Poinsot, Flow forcing techniques for numerical simulation of combustion instabilities, Combust. Flame 131 (4) (2002) 371–385.
[13] W. Polifke, C. Wall, Non-reflecting boundary conditions for acoustic transfer matrix estimation with LES, in: Proceedings of the Summer Program 2002, Center for Turbulence Research, Stanford, USA, 2002, URL: ctr.stanford.edu/Summer02/polifke.pdf.
[14] S.W. Yuen, A. Gentemann, W. Polifke, Investigation of the influence of boundary conditions on system identifiability using real time system modeling, in: Proceedings of the 11th International Congress on Sound and Vibration (ICSV11), IIAV, Saint-Petersburg, Russia, 2004, pp. 3501–3508.
[15] W. Polifke, A. Poncet, C.O. Paschereit, K. Döbbeling, Reconstruction of acoustic transfer matrices by instationary computational fluid dynamics, J. Sound Vibr. 245 (3) (2001) 483–510.
[16] W. Polifke, Numerical techniques for identification of acoustic multi-poles, in: Advances in Aeroacoustics and Applications, VKI LS 2004-05, Von Karman Institute, Brussels, BE, 2004.
[17] P. Moin, K. Squires, W. Cabot, S. Lee, A dynamic subgrid-scale model for compressible turbulence and scalar transport, Phys. Fluids A 3 (11) (1991) 2746–2757.
[18] C. Wall, C.D. Pierce, P. Moin, A semi-implicit method for resolution of acoustic waves in low Mach number flows, J. Comput. Phys. 181 (2002) 545.
[19] C.D. Pierce, Progress-variable approach for large-eddy simulation of turbulent combustion. Ph.D. Thesis, Stanford University, Stanford, CA, 2001.
[20] C.D. Pierce, P. Moin, Progress-variable approach for large-eddy simulation of turbulent combustion, Tech. Rep. TF-80, CTR, Stanford University, Stanford, CA, 2001.
[21] J. Kopitz, E. Bröker, W. Polifke, Characteristics-based filter for identification of acoustic waves in numerical simulation of turbulent compressible flow, in: Proceeding of the 12th International Congress on Sound and Vibration (ICSV12), vol. 389, IIAV, Lisbon, Portugal, 2005.
[22] M. Besson, P. Bruel, J.L. Champion, B. Deshaies, Experimental analysis of combusting flow developing over a plane-symmetric expansion, in: AIAA 99-0412, 1999.
[23] C. Wall, Numerical methods for large eddy simulation of acoustic combustion instabilities. Ph.D. Thesis, Stanford University, 2005.